Nuclear Medicine and Biology 59 (2018) 16–21

Contents lists available at ScienceDirect

Nuclear Medicine and Biology

journal homepage: www.elsevier.com/locate/nucmedbio

Development of radioiodine labeled acetaminophen for specific, high-contrast imaging of malignant melanoma☆

Wen Jing Zhu [a], Masato Kobayashi [b,*], Kohei Yamada [c], Kodai Nishi [d], Kotaro Takahashi [a], Asuka Mizutani [e,f], Ryuichi Nishii [g], Leo G. Flores II [h], Naoto Shikano [i], Munetaka Kunishima [c], Keiichi Kawai [a,j]

[a] Department of Health Sciences, College of Medical, Pharmaceutical and Health Sciences, Kanazawa University, Kanazawa, Japan
[b] Wellness Promotion Science Center, College of Medical, Pharmaceutical and Health Sciences, Kanazawa University, Kanazawa, Japan
[c] Department of Pharmaceutical Sciences, College of Medical, Pharmaceutical and Health Sciences, Kanazawa University, Kanazawa, Japan
[d] Department of Radioisotope Medicine, Atomic Bomb Disease Institute, Nagasaki University, Nagasaki, Japan
[e] Graduate School of Medicine, Division of Health Science, Osaka University, Osaka, Japan
[f] Department of Radiology, Kanazawa University Hospital, Kanazawa, Japan
[g] Molecular Imaging Center, National Institute of Radiological Sciences, Chiba, Japan
[h] Department of Cancer Systems Imaging, University of Texas M.D. Anderson Cancer Center, Houston, TX, USA
[i] Department of Radiological Sciences, Ibaraki Prefectural Sciences of Health Sciences, Ibaraki, Japan
[j] Biomedical Imaging Research Center, University of Fukui, Fukui, Japan

ARTICLE INFO

Article history:
Received 4 July 2017
Received in revised form 21 December 2017
Accepted 26 December 2017

Keywords:
Malignant melanoma
Acetaminophen
Radioiodine
SPECT imaging
Tyrosinase

ABSTRACT

Introduction: Due to its poor prognosis, specific imaging for early detection of malignant melanoma is strongly desired. Although radioiodine labeled 4-hydroxyphenylcysteamine, which we previously developed, has good affinity for tyrosinase, an enzyme in the melanin metabolic pathway, image contrast of the melanoma:organ ratios is not sufficiently high for detection of primary melanoma and metastases at early injection times. In this study, we developed radioiodine labeled acetaminophen (I-AP) for specific, high-contrast imaging of malignant melanoma.

Methods: Radioiodine-125-labeled AP (^{125}I-AP) was prepared using the chloramine-T method under no carrier-added conditions. Accumulation of radioactivity and the mechanism were evaluated in vitro using B16 melanoma cells incubated with ^{125}I-AP or ^{14}C(U)-labeled AP (^{14}C-AP) with and without L-tyrosine as a substrate of tyrosinase, phenylthiourea as an inhibitor of tyrosinase, and thymidine as an inhibitor of DNA polymerase. The biological distribution of radioactivity in B16 melanoma-bearing mice was evaluated to determine the accumulation of ^{125}I-AP. The stability of ^{125}I-AP over time was evaluated in mice.

Results: The labeling efficiency and radiochemical purity of ^{125}I-AP were >80% and 95%, respectively. Accumulation of ^{125}I-AP was higher than that of ^{14}C-AP at 60 min of incubation in vitro. The affinity of ^{14}C-AP for tyrosinase and DNA polymerase was higher than that of ^{125}I-AP, whereas the V_{max} of ^{125}I-AP was higher than that of ^{14}C-AP. ^{125}I-AP showed the highest accumulation in the gall bladder, and clearance from the blood and kidney was rapid. Melanoma:muscle and melanoma:normal skin ratios of ^{125}I-AP for imaging contrast were the highest at 15 min after injection, whereas the melanoma:blood and melanoma:bone ratios gradually increased over time. ^{125}I-AP remained stable for 60 min after injection in mice.

Conclusions: ^{125}I-AP has affinity for tyrosinase and high image contrast at early time points after injection. Therefore, ^{123}I-AP imaging has great potential for specific, high-contrast detection of malignant melanoma.

Advances in knowledge: ^{123}I-AP will provide specific, high-contrast imaging for malignant melanoma at early injection times.

Implications for patient care: ^{123}I-AP has good potential for the diagnosis of malignant melanoma compared with ^{123}I-labeled 4-hydroxyphenylcysteamine, which we previously developed.

1. Introduction

The 5-year survival rate with stage IV metastatic melanoma is currently <20% because no effective treatments have been established [1, 2]. Because survival is associated with an early stage at detection, specific detection of the primary and metastatic malignant melanoma tumors

☆ Financial support: This study was partly funded by Grants-in-Aid for Scientific Research from the Japan Society for the Promotion of Science (Nos. 25293260, 15K09949, 15K15452, and 16KK0200) and the Program of the Network-Type Joint Usage/Research Center for Radiation Disaster Medical Science of Hiroshima University, Nagasaki University, and Fukushima Medical University (105-N).

* Corresponding author at: Wellness Promotion Science Center, College of Medical, Pharmaceutical and Health Science, Kanazawa University, 5-11-80 Kodatsuno, Kanazawa 920-0942, Japan.
E-mail address: kobayasi@mhs.mp.kanazawa-u.ac.jp (M. Kobayashi).

https://doi.org/10.1016/j.nucmedbio.2017.12.008
0969-8051/

is strongly desired. Melanomas develop due to an increase in activity of the melanin biosynthetic pathway in melanin-producing cells (melanocytes) [3]. Melanin biosynthesis involves conversion of tyrosine to dopa, and then subsequent oxidation of dopa to dopaquinone by the tyrosinase enzyme. Therefore, radiopharmaceuticals with affinity for tyrosinase are potential specific imaging agents.

Single photon emission computed tomography (SPECT) [4–14] and positron emission tomography (PET) imaging [14–16] have been used to detect the primary melanoma and metastases. With SPECT imaging, some radiopharmaceuticals (melanocortin-1 receptor-targeting peptide [11] and iodobenzamide [7, 12, 13]) can image melanomas by targeting tumor receptors. Melanocortin-1 receptor-targeting peptide may not be useful for clinical imaging of melanoma because of high renal accumulation, although methods to reduce kidney uptake have been suggested [11]. ^{123}I-*N*-(2-diethylaminoethyl)-2-iodobenzamide, an iodobenzamide derivative, showed low uptake for detection of melanoma metastases in a clinical study [13]. Therefore, imaging with this derivative would require a very high radiation dose in clinical studies. Thus, these radiopharmaceuticals that allow specific imaging of melanoma have not been fully developed. On the other hand, ^{18}F-fluorodeoxyglucose (FDG)-PET imaging was useful for detection of the primary melanoma and metastases, but FDG-PET does not have high enough specificity to detect melanoma [14, 15], and the availability of PET is still lower than that of SPECT because many facilities do not have a cyclotron for synthesis of PET tracers.

We previously developed ^{125}I-labeled 4-hydroxyphenyl-L-cysteine [4] and radioiodine labeled 4-hydroxyphenylcysteamine (I-PCA) [5] that have good affinity for tyrosinase. However, the image contrast of the melanoma:organ ratios might not be sufficiently high for detection of primary and metastatic melanoma at early injection times. Acetaminophen (AP) for chemotherapy is selectively bioactivated by tyrosinase to form active quinone metabolites that are toxic to melanoma cells. The selective toxicity and efficacy of AP for melanoma has been previously reported in B16 melanoma tumor-bearing C57BL/6 mice [17, 18] . However, the effect of chemotherapeutic drugs such as AP cannot be visualized. We hypothesize that AP may be a good molecule for detection of primary and metastatic melanoma. In this study, we developed radioiodine labeled AP (I-AP) (Fig. 1), which is a specific imaging radiotracer of malignant melanoma.

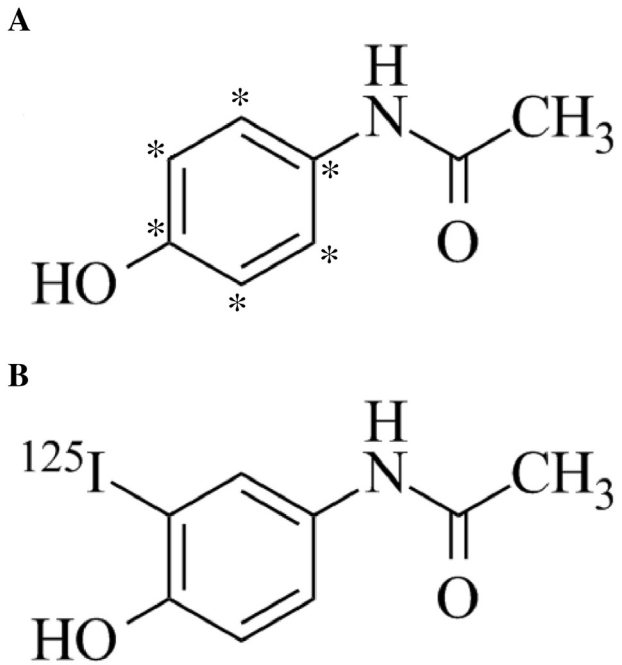

Fig. 1. Structures of ^{14}C-AP (A) and ^{125}I-AP (B). On the ^{14}C-AP structure (A), * means ^{14}C labeling.

2. Materials and methods

2.1. Preparation of ^{125}I-AP and ^{127}I-AP

Radioiodine-125-labeled AP (Nakalai Tesque, Kyoto, Japan) (^{125}I-AP) was synthesized with the chloramine-T (Nakalai Tesque) method under no carrier-added conditions [4, 5]. In brief, 4 mM chloramine-T was added to a mixture of 10 mM AP in ethanol (≥99.5%, Sigma-Aldrich, St. Louis, MO) and 3.7–37 MBq Na^{125}I (American Radiolabeled Chemicals, Inc., St. Louis, MO) in the absence of carriers. Thirty minutes later, 280 mM sodium sulfite (Sigma-Aldrich) in 0.05 M phosphate buffer (pH 6.2) was added to stop the reaction. The labeling efficiency of ^{125}I-AP was determined with thin-layer chromatography (TLC, Silica gel 60 F_{254}; Merck Millipore, Darmstadt, Germany) with the solvent system of hexane:ethylacetate:diethylether at 1:4:1 (R_f value: ^{125}I-AP; 0.15–0.25, $^{125}I^-$; 0.0) and/or methanol:acetic acid at 100:1 (R_f value: ^{125}I-AP; 0.70–0.80, $^{125}I^-$; 0.90–0.95). The R_f value for TLC and the peak position for high performance liquid chromatography (HPLC) of ^{125}I-AP were confirmed using Na^{127}I-labeled AP (^{127}I-AP). To synthesize ^{127}I-AP, AP in a mixture of 0.1 M $CHCl_3$ and 0.8 M K_2CO_3 was reacted with 0.8 M Na^{127}I in 0.1 M ethanol at room temperature. About 10 min later, the solution was cooled to about 0 °C, and then 0.1 M $CHCl_3$ was added to stop the reaction. After washing with 1 M HCl and brine, the final solution was dried by Na_2SO_4. ^{127}I-AP was obtained by the preparative TLC method. The structure of ^{127}I-AP was confirmed by gas chromatography-mass spectrometry (MS, JMS-700 electron impact; Japan Electron Optics Laboratory, Tokyo, Japan).

The radiochemical purity of ^{125}I-AP was examined with HPLC (Hitachi, Ibaraki, Japan) using a 5C18-MS-II column (Cosmosil, Nakalai Tesque), a combination gamma counter, and 225 nm ultraviolet light. The initial solvent was methanol:50 mM KH_2PO_4 (pH 4.7) at 20:80 for the first 10 min after injection, and then the same solvent at a 50:50 ratio for the next 10 min as the eluent at a flow rate of 1.0 mL/min.

2.2. B16 melanoma cells

Mouse skin melanoma B16 cells were obtained from RIKEN Cell Bank in Japan and cultured in Dulbecco's Modified Eagle's Medium (Sigma-Aldrich) supplemented with 10% fetal bovine serum (Dainippon Sumitomo, Osaka, Japan) at 37 °C in a 5% CO_2 incubator.

2.3. In vitro assays with B16 melanoma cells without and with a substrate and inhibitors

In vitro assays were performed using the methods of Kobayashi et al., with some modifications [5, 19]. ^{14}C(U)-labeled AP (^{14}C-AP) was purchased from American Radiolabeled Chemicals Inc., and ^{125}I-AP was synthesized by the method described above. Briefly, B16 melanoma cells were seeded into 24-well cell culture multiwell plates at a density of 5×10^5 cells/well. Assays were conducted 24 h after seeding. After the culture medium was removed, each well was incubated with 0.5 M HEPES buffer (pH 7.4) for 10 min at 37 °C. Then, 18.5 kBq/well ^{125}I-AP or ^{14}C-AP was added and incubated for 5, 15, 30, 60, and 120 min at 37 °C as the control condition. Michaelis-Menten analyses were carried out using AP as a parent compound, L-tyrosine (Sigma-Aldrich) as a tyrosinase substrate, N-phenylthiourea (PTU; Sigma-Aldrich) as an inhibitor of tyrosinase, and thymidine (Nakalai Tesque) as an inhibitor of DNA polymerase at concentrations of 0, 0.01, 0.1, 0.5, 1, 1.5, 2.0, 3.0, 4.0, and 5.0 mM [20, 21]. B16 melanoma cells were incubated for 30 min with ^{125}I-AP or ^{14}C-AP plus one of these inhibitors at 37 °C. At the end of the incubation, each well was rapidly washed twice with 500 μL of 0.5 M HEPES buffer. Cells were then solubilized in 500 μL of 0.1 M NaOH. The ^{125}I-AP radioactivity that accumulated in B16

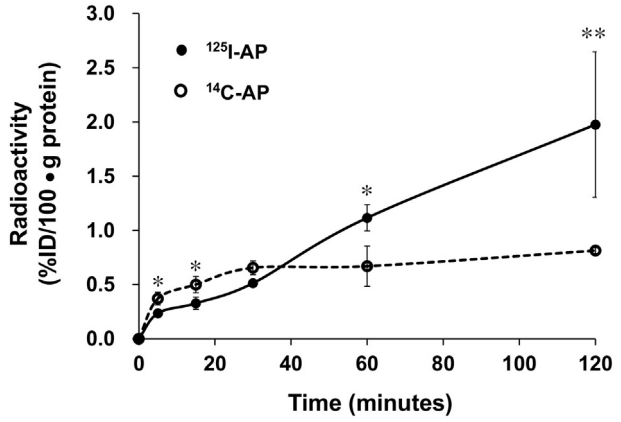

Fig. 2. In vitro assays of ^{14}C-AP and ^{125}I-AP in B16 melanoma cells. 18.5 kBq/well ^{125}I-AP (mass; 278.1) or 18.5 kBq/well ^{14}C-AP (mass; 151.2) was incubated for 5, 15, 30, 60, and 120 min. ^{14}C-AP was taken up earlier into the tumor cells and reached a steady state after about 30 min of incubation. In contrast, ^{125}I-AP was taken up gradually, and the accumulation of ^{125}I-AP exceeded that of ^{14}C-AP after about 60 min of incubation. Data are the mean ± standard deviation. $^{**}P < .01$ and $^{*}P < .05$ between ^{125}I-AP and ^{14}C-AP.

melanoma cells was measured with a gamma counter (ARC-380; Hitachi-Aloka Medical, Tokyo, Japan), and that of ^{14}C-AP was mixed with scintillation fluid (Ultima Gold, PerkinElmer, Inc., Waltham, MA) and measured with a liquid scintillation counter (LSC-5100; Hitachi-Aloka Medical). B16 melanoma cells were detached with trypsin, and the protein in the cells was measured using a protein assay. All experimental conditions were examined with quadruplicate assays.

2.4. Biological distribution of ^{125}I-AP in B16 melanoma-bearing mice

All animal studies were conducted following approval by the Animal Care Committee of Kanazawa University. C57BL6 male mice (5 weeks old) were transplanted with B16 melanoma cells (5×10^5 cells/100 μL) into the thigh of the mice [6]. The tumors appeared and increased gradually after about 10 days. The mice were housed for 2 weeks under a 12-h light/12-h dark cycle with free access to food and water. Before the bio-distribution experiment, B16 melanoma-bearing mice were fasted overnight with only water available. ^{125}I-AP (37 kBq) was injected into the tail vein of B16 melanoma-bearing mice, and five mice each were killed at 5, 10, 15, 30, and 60 min after injection. After blood sampling via cardiocentesis, the brain, pancreas, spleen, stomach, small intestine, kidney, liver, heart, lung, thyroid, gall bladder, skin, muscle, bone, and melanoma were removed. Radioactivity in weighed tissue samples was measured using a gamma counter (ARC-380; Aloka, Tokyo, Japan). Data were expressed in terms of the injected dose (%ID/organ) for stomach, small intestine, and thyroid and injected dose per weight of tissues (%ID/g tissue) for the other organs.

$$\%\text{ID/organ} = (\text{radioactivity of tissue [cpm]}/\text{radioactivity of injection [cpm]}) \times 100$$

$$\%\text{ID/g} = (\%\text{ID/weight of tissues [g]}) \times 100$$

2.5. Stability analysis in mice

^{125}I-AP was prepared to a specific activity of 37 MBq/mL by addition of saline. Fasted C57BL6 male mice (6–8 weeks old) were administered ^{125}I-AP via the tail vein (3.7 MBq/mouse). At 5, 10, 15, 30, and 60 min after injection, mice were euthanized with isoflurane (n = 3), and blood and liver were collected and analyzed with TLC. Briefly, heparin was added to 300 μL blood, which was centrifuged at 18,000 ×*g* at 4 °C for 5 min. A total of 30 μL perchloric acid was added to the supernatant, which was centrifuged again, after which the final supernatant was spotted onto the TLC plate as plasma. Krebs-Ringer phosphate buffer (pH 7.4) was added to the liver samples, followed by homogenization with an ultrasonic homogenizer (SONIFIER250, Branson, MO, USA). Then, ethanol was added to the homogenate to remove proteins, and the sample was centrifuged at 18,000 ×*g* at 4 °C for 5 min. The final supernatant was spotted onto the TLC plate, and the TLC spots were developed using the above-mentioned solvents. After development and complete drying, the TLC plates were cut into 21 fractions, and the radioactivity associated with each fraction was quantified using a γ-ray counter. The fraction ratios of $^{125}I^-$ and ^{125}I-AP were calculated by dividing the radioactive counts for each fraction by the total radioactivity count.

2.6. Statistical analysis

Data are presented as mean and standard deviation (SD). *P* values were calculated using a two-tailed Student's *t*-test. Results were considered to be significant at $P < 0.05$.

3. Results

3.1. Preparation of ^{125}I-AP

MS data revealed an MH(+) of 278, which matched the calculated MH(+) of 278 for $C_8H_8INO_2$. With TLC analysis, using the results of the R_f values for ^{127}I-AP, the R_f values of ^{125}I-AP and $^{125}I^-$ were 0.15-0.25 and 0.00, respectively. ^{125}I-AP was labeled with an efficiency of >80%. With HPLC analysis, the retention times were about 3 min for

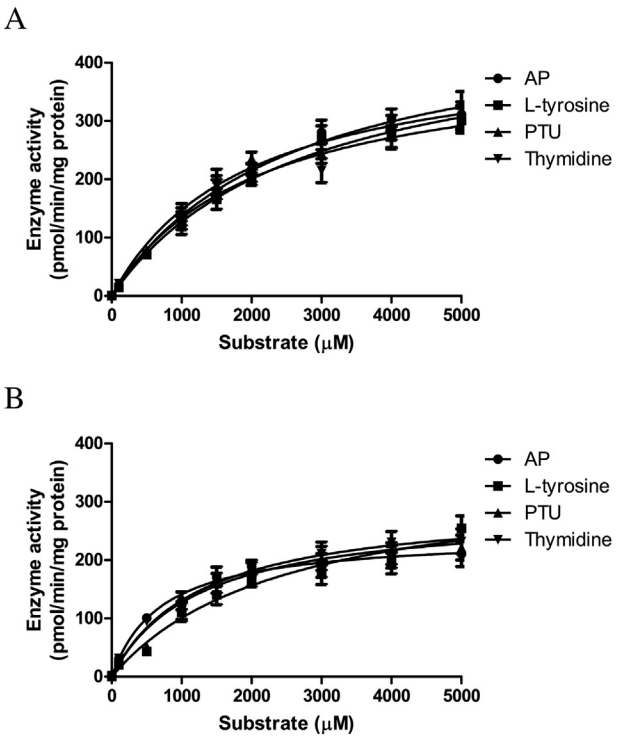

Fig. 3. Michaelis-Menten analyses using ^{125}I-AP (A) or ^{14}C-AP (B) with cold AP, L-tyrosine, PTU, and thymidine in B16 melanoma cells. K_m values of ^{125}I-AP with AP, L-tyrosine, PTU, and thymidine were 2.56 ± 0.31, 2.73 ± 0.39, 1.93 ± 0.29, and 2.10 ± 0.41 mM, respectively, whereas those of ^{14}C-AP were 0.71 ± 0.08, 2.47 ± 0.67, 1.23 ± 0.30, and 1.26 ± 0.18 mM, respectively. V_{max} values of ^{125}I-AP with AP, L-tyrosine, PTU, and thymidine were 490.3 ± 27.3, 473.5 ± 32.8, 433.1 ± 27.0, and 413.9 ± 35.2 pmol/min/mg protein, respectively, whereas those of ^{14}C-AP were 242.3 ± 7.6, 349.5 ± 44.2, 284.7 ± 23.7, and 296.2 ± 15.1 pmol/min/mg protein, respectively.

Table 1
Biological distribution of ^{125}I-AP in B16 melanoma-bearing C57BL6 mice.

Organ or tumor	Time (minutes)				
	5	10	15	30	60
Blood	13.51 ± 1.0	8.92 ± 1.4	6.42 ± 1.1	2.82 ± 0.0	1.10 ± 0.3
Brain	0.64 ± 0.1	0.26 ± 0.1	0.21 ± 0.0	0.09 ± 0.0	0.05 ± 0.0
Pancreas	3.50 ± 0.5	4.25 ± 0.2	2.96 ± 0.3	1.03 ± 0.3	1.92 ± 1.7
Spleen	2.95 ± 0.3	2.97 ± 0.2	2.12 ± 0.4	0.73 ± 0.2	0.63 ± 0.1
Stomach[a]	0.78 ± 0.0	0.69 ± 0.2	1.00 ± 0.2	1.21 ± 0.1	0.76 ± 0.1
Small intestine[a]	6.89 ± 0.3	6.08 ± 0.1	6.53 ± 0.6	3.31 ± 0.3	8.93 ± 2.2
Kidney	17.32 ± 2.1	12.19 ± 2.3	9.94 ± 2.4	3.39 ± 0.7	1.30 ± 0.2
Liver	5.20 ± 0.6	4.51 ± 0.9	3.50 ± 0.6	1.88 ± 1.6	1.26 ± 0.5
Heart	4.34 ± 0.5	3.28 ± 0.6	2.08 ± 0.3	0.87 ± 0.2	0.31 ± 0.0
Lung	13.09 ± 0.1	8.24 ± 1.5	6.26 ± 0.7	3.42 ± 0.7	1.68 ± 0.0
Thyroid[a]	0.08 ± 0.0	0.08 ± 0.0	0.07 ± 0.0	0.05 ± 0.0	0.01 ± 0.0
Gall bladder	22.28 ± 8.4	27.77 ± 2.0	18.94 ± 6.4	72.06 ± 20.1	47.34 ± 17.2
Skin	4.21 ± 0.8	4.24 ± 0.7	3.05 ± 0.3	2.38 ± 0.2	0.96 ± 0.0
Muscle	1.71 ± 0.5	1.24 ± 0.8	0.79 ± 0.1	0.56 ± 0.8	0.28 ± 0.3
Bone	2.01 ± 0.7	2.07 ± 0.3	1.35 ± 0.5	0.48 ± 0.4	0.18 ± 0.0
Melanoma	2.43 ± 0.1	3.61 ± 0.2	4.65 ± 1.6	2.30 ± 0.2	1.06 ± 0.1

Percent injected dose per g tissue (%ID/g), mean ± standard deviation of data from five mice.
[a] %ID/organ was calculated by dividing the radioactivity in the tissue by the radioactivity that was injected.

^{125}I$^-$ and 16–17 min for ^{127}I-AP and ^{125}I-AP. Non-carrier-added ^{125}I-AP was obtained with a radiochemical purity of >95% after purification.

3.2. In vitro assays with B16 melanoma cells without and with a substrate and inhibitors

The comparison of the accumulation of ^{125}I-AP and ^{14}C-AP in B16 melanoma cells is shown in Fig. 2. ^{125}I-AP was gradually taken up by the cells, and accumulation of ^{125}I-AP exceeded that of ^{14}C-AP after about 60 min of incubation. In contrast, ^{14}C-AP was taken up into the tumor cells early and reached a steady-state after about 30 min of incubation.

Fig. 3 shows the Michaelis-Menten analyses using ^{125}I-AP (A) or ^{14}C-AP (B) with cold AP, L-tyrosine, PTU, and thymidine in B16 melanoma cells. K_m values of ^{125}I-AP with AP, L-tyrosine, PTU, and thymidine were 2.56 ± 0.31, 2.73 ± 0.39, 1.93 ± 0.29, and 2.10 ± 0.41 mM, respectively, whereas those of ^{14}C-AP were 0.71 ± 0.08, 2.47 ± 0.67, 1.23 ± 0.30, and 1.26 ± 0.18 mM, respectively. V_{max} values of ^{125}I-AP with AP, L-tyrosine, PTU, and thymidine were 490.3 ± 27.3, 473.5 ± 32.8, 433.1 ± 27.0, and 413.9 ± 35.2 pmol/min/mg protein, respectively, whereas those of ^{14}C-AP were 242.3 ± 7.6, 349.5 ± 44.2, 284.7 ± 23.7, and 296.2 ± 15.1 pmol/min/mg protein, respectively.

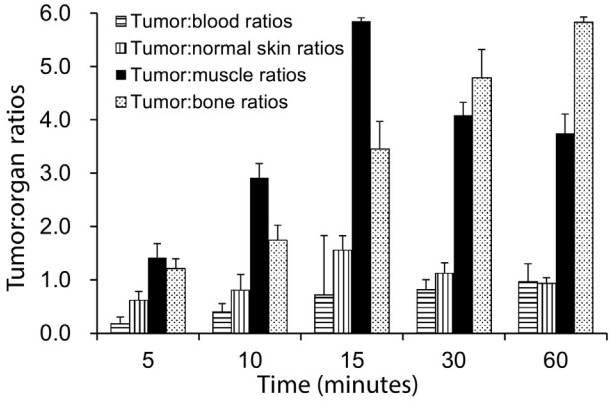

Fig. 4. Ratios of melanoma:blood, melanoma:skin, melanoma:muscle, and melanoma:bone in B16 melanoma-bearing C57BL6 mice at 5, 10, 15, 30, and 60 min after 37 kBq ^{125}I-AP injection. The melanoma:muscle and melanoma:normal skin ratios were the highest at 15 min after injection, whereas the melanoma:blood and melanoma:bone ratios increased over time. All values were obtained using five mice each. Data are the mean ± standard deviation.

3.3. Biological distribution of ^{125}I-AP in B16 melanoma-bearing mice

Table 1 summarizes the biological distribution of ^{125}I-AP in B16 melanoma-bearing mice. Accumulation of ^{125}I-AP in the melanoma was the highest at 15 min after injection. ^{125}I-AP accumulation was highest in the gall bladder, and clearance of ^{125}I-AP from the blood and kidney was rapid.

Fig. 4 shows the melanoma:blood ratios, melanoma:normal skin ratios, melanoma:muscle ratios, and melanoma:bone ratios in B16 melanoma-bearing mice at each time after injection. The melanoma:muscle ratios and melanoma:normal skin ratios were the highest at 15 min after injection, whereas the melanoma:blood ratios and melanoma:bone ratios gradually increased over time.

3.4. Stability analysis in mice

Table 2 shows the stability over time of ^{125}I-AP in blood and liver of mice. In the blood, ^{125}I-AP showed high stability over time, but in the liver, ^{125}I-AP was slightly metabolized at 5 min after injection. Then, ^{125}I-AP remained stable during 60 min after injection.

4. Discussion

Specific imaging of primary and metastatic melanoma is important for patient survival because detection and treatment at earlier stages are more effective. As general clinical examination methods for detection of melanoma, visual inspection [22], dermoscopy [23], and ultrasonography [23, 24] are useful for detection of mainly primary melanoma, whereas computed tomography [25, 26] and magnetic resonance imaging [25] are effective for detection of primary and metastatic melanoma in the whole body. Although these methods are very useful for finding structural changes in melanoma, detection of primary and metastatic melanoma at earlier stages may be insufficient. Nuclear medicine imaging, which we focused on in this study, can detect biological functional changes in melanoma before structural changes in the melanoma occur. We developed SPECT imaging radiotracers with high availability and specificity for detection of the primary melanoma and metastases.

Table 2
Stability analysis of ^{125}I-AP in blood and liver of mice.

Time (minutes)	5	10	15	30	60
Blood (%)	94.8 ± 7.2	94.4 ± 5.4	94.2 ± 8.2	93.8 ± 1.4	94.1 ± 5.1
Liver (%)	90.9 ± 6.5	89.3 ± 5.1	90.6 ± 6.8	89.9 ± 4.7	88.2 ± 5.5

All data are the mean ± standard deviation from triplicate measurements.

Tyrosine analogues, which are substrates of the tyrosinase enzyme, are good candidates for drugs for melanoma-targeting chemotherapies [27]. In addition, the affinity of tyrosine analogues for detection of elevated tyrosinase enzyme activity in melanin biosynthesis indicates the possibility of application for specific detection of melanoma. Although we previously developed two radiotracers, which are good substrates for tyrosinase and are retained longer in malignant melanoma cells [4, 5], improved image contrast due to the tumor:organ ratios is required for clinical imaging of melanoma for high-throughput examination.

Vad et al. reported that AP has affinity for tyrosinase in melanoma cells [17, 18]. We hypothesized that ^{125}I-AP would be a useful SPECT imaging agent for specific detection of melanoma. In our previous study, iodination of AP was estimated at the ortho position to the 4-hydroxyl group [4, 5, 28]. In our in vitro study, ^{125}I-AP accumulation was significantly higher than that of ^{14}C-AP at 60 min of incubation, although accumulation of ^{14}C-AP was higher than that of ^{125}I-AP at early incubation times (Fig. 2). As the in vitro study was conducted using equal amounts of radioactivity with about 300-fold different specific activities (^{14}C-AP: 1.85–2.22 GBq/mmol and ^{125}I-AP: about 600 GBq/mmol), the relative uptake velocities into melanoma cells may be much different. In our previous study, although ^{125}I-L-tyrosine had higher affinity for system L amino acid transporters than ^{14}C-L-tyrosine due to the effect of radioiodine labeling, accumulation of ^{14}C-L-tyrosine was higher than that of ^{125}I-L-tyrosine at early incubation times [28]. In this study, we estimate that accumulation of ^{14}C-AP was higher than that of ^{125}I-AP due to the effect of the accumulation mechanism.

In Fig. 3, Michaelis-Menten analyses were performed in B16 melanoma cells using ^{125}I-AP (A) or ^{14}C-AP (B) with cold AP as the parent compound, L-tyrosine and PTU as a substrate and inhibitor of tyrosinase, respectively, and thymidine as an inhibitor of DNA polymerase. K_m values of ^{125}I-AP with AP, L-tyrosine, PTU, and thymidine were 2.56 ± 0.31, 2.73 ± 0.39, 1.93 ± 0.29, and 2.10 ± 0.41 mM, respectively, whereas those of ^{14}C-AP were 0.71 ± 0.08, 2.47 ± 0.67, 1.23 ± 0.30, and 1.26 ± 0.18 mM, respectively. Thus, the affinity of ^{14}C-AP for tyrosinase and DNA polymerase was higher than that of ^{125}I-AP in B16 melanoma cells. From these results, we estimated that accumulation of ^{14}C-AP was higher than that of ^{125}I-AP at early incubation times (Fig. 2). V_{max} values of ^{125}I-AP with AP, L-tyrosine, PTU, and thymidine were 490.3 ± 27.3, 473.5 ± 32.8, 433.1 ± 27.0, and 413.9 ± 35.2 pmol/min/mg protein, respectively, whereas those of ^{14}C-AP were 242.3 ± 7.6, 349.5 ± 44.2, 284.7 ± 23.7, and 296.2 ± 15.1 pmol/min/mg protein, respectively. Thus, the V_{max} of ^{125}I-AP for tyrosinase and DNA polymerase was higher than that of ^{14}C-AP in B16 melanoma cells. From these results, we also estimated that ^{125}I-AP accumulation was significantly higher than that of ^{14}C-AP at 60 min of incubation (Fig. 2).

In the biological distribution experiment with B16 melanoma-bearing mice (Table 1), accumulation of ^{125}I-AP in the melanoma was the highest at 15 min after injection, whereas ^{125}I-PCA showed the highest accumulation at 30 min after injection [5]. Therefore, ^{125}I-AP may allow earlier acquisition than ^{125}I-PCA in whole body imaging. In addition, ^{125}I-AP was washed out faster from blood and was excreted as quickly by the kidney as ^{125}I-PCA [5]. The washout of ^{125}I-AP was also faster than that of other radioligands for melanoma imaging [7, 10–12]. Melanoma:muscle and melanoma:normal skin ratios for imaging contrast were the highest at 15 min after injection (Fig. 4). The average melanoma:muscle ratio (5.9) for primary melanoma and melanoma:bone ratio (3.5) for melanoma metastases of ^{125}I-AP were significantly greater than those of ^{125}I-PCA (2.1, 1.5, respectively), whereas the average melanoma:blood (0.7) and melanoma:normal skin ratios (1.5) for ^{125}I-AP were similar to those of ^{125}I-PCA (0.8 and 1.8, respectively) [5]. From results of these melanoma:organ ratios, ^{125}I-AP is likely to be an effective radiotracer for specific, high-contrast imaging of malignant melanoma. However, radioiodide-131-labeled AP may not be applicable in radionuclide therapy because the melanoma:muscle and melanoma:normal skin ratios gradually decreased 15 min after injection.

Regarding the stability over time, ^{125}I-AP was quite stable with about 95% in mouse blood and 90% in mouse liver remaining 60 min after injection. ^{125}I-AP is minimally deiodinated because it does not accumulate in the thyroid, and thus, metabolites of ^{125}I-AP may have little influence on accumulation of ^{125}I-AP in melanoma.

5. Conclusion

^{125}I-AP has affinity for tyrosinase and high imaging contrast at early times after injection. Therefore, ^{123}I-AP imaging has great potential for specific, high-contrast imaging of malignant melanoma.

Conflict of interest statement

There is no conflict of interest.

Acknowledgments

The authors would like to thank Mikie Ohtaki and the other laboratory staff of Kanazawa University. This study was partly funded by Grants-in-Aid for Scientific Research from the Japan Society for the Promotion of Science (Nos. 25293260, 15K09949, and 15K15452) and the Program of the Network-Type Joint Usage/Research Center for Radiation Disaster Medical Science of Hiroshima University, Nagasaki University, and Fukushima Medical University.

References

[1] American Cancer Society. What Are the Key Statistics About Melanoma? http://www.cancer.org/cancer/skincancer-melanoma/detailedguide/melanoma-skin-cancer-key-statistics. [Accessed 2017].
[2] Cancer Research UK. Skin cancer incidence statistics. http://www.cancerresearchuk.org/cancer-info/cancerstats/types/skin/incidence/uk-skin-cancer-incidence-statistics. [Accessed 2017].
[3] Pawelek JM. Factors regulating growth and pigmentation of melanoma cells. J Invest Dermatol 1976;66:201–9.
[4] R. Nishii, K Kawai, L. Garcia Flores II, Kataoka H, Jinnouchi S, Nagamachi S, et al. A novel radiopharmaceutical for detection of malignant melanoma, based on melanin formation: 3-iodo-4-hydroxyphenyl-L-cysteine. Nucl Med Commun 2003;24:575–82.
[5] Kobayashi M, Nishii R, Shikano N, Flores II LG, Mizutani A, Ogai K, et al. Development of radioiodine-labeled 4-hydroxyphenylcysteamine for specific diagnosis of malignant melanoma. Nucl Med Biol 2015;42:536–40.
[6] Moreau MF, Papon J, Labarre P, Moins N, Borel M, Bayle M, et al. Synthesis, in vitro binding and biodistribution in B16 melanoma-bearing mice of new iodine-125 spermidine benzamide derivatives. Nucl Med Biol 2005;32:377–84.
[7] Michelot JM, Moreau MF, Labarre PG, Madelmont JC, Veyre AJ, Papon JM, et al. Synthesis and evaluation of new iodine-125 radiopharmaceuticals as potential tracers for malignant melanoma. J Nucl Med 1991;32:1573–80.
[8] Coenen HH, Dutschka K, Müller SP, Geworski L, Farahati J, Reiners CN. c.a. radiosynthesis of [^{123},^{124}I]beta-CIT, plasma analysis and pharmacokinetic studies with SPECT and PET. Nucl Med Biol 1995;22:977–84.
[9] Labarre P, Papon J, Moreau MF, Moins N, Veyre A, Madelmont JC. Evaluation in mice of some iodinated melanoma imaging agents using cryosectioning and multi-wire proportional counting. Eur J Nucl Med 1999;26:494–8.
[10] John CS, Bowen WD, Saga T, Kinuya S, Vilner BJ, Baumgold J, et al. A malignant melanoma imaging agent: synthesis, characterization, in vitro binding and biodistribution of iodine-125-(2-piperidinylaminoethyl)4-iodobenzamide. J Nucl Med 1993;34:2169–75.
[11] Miao Y, Owen NK, Whitener D, Gallazzi F, Hoffman TJ, Quinn TP. In vivo evaluation of ^{188}Re-labeled alpha-melanocyte stimulating hormone peptide analogs for melanoma therapy. Int J Cancer 2002;101:480–7.
[12] Pham TQ, Berghofer P, Liu X, Chapman J, Greguric I, Mitchell P, et al. Preparation and biologic evaluation of a novel radioiodinated benzylpiperazine, ^{123}I-MEL037, for malignant melanoma. J Nucl Med 2007;48:1348–56.
[13] Cachin F, Miot-Noirault E, Gillet B, Isnardi V, Labeille B, Payoux P, et al. ^{123}I-BZA2 as a melanin-targeted radiotracer for the identification of melanoma metastases: results and perspectives of a multicenter phase III clinical trial. J Nucl Med 2014;55:15–22.
[14] Kato K, Kubota T, Ikeda M, Tadokoro M, Abe S, Nakano S, et al. Low efficacy of ^{18}F-FDG PET for detection of uveal malignant melanoma compared with ^{123}I-IMP SPECT. J Nucl Med 2006;47:404–9.
[15] Bastiaannet E, Wobbes T, Hoekstra OS, van der Jagt EJ, Brouwers AH, Koelemij R, et al. Prospective comparison of [^{18}F]fluorodeoxyglucose positron emission tomography and computed tomography in patients with melanoma with palpable lymph node metastases: diagnostic accuracy and impact on treatment. J Clin Oncol 2009;27:4774–80.
[16] Rizzo-Padoin N, Chaussard M, Vignal N, Kotula E, Tsoupko-Sitnikov V, Vaz S, et al. [^{18}F]MEL050 as a melanin-targeted PET tracer: fully automated radiosynthesis and

comparison to ^{18}F-FDG for the detection of pigmented melanoma in mice primary subcutaneous tumors and pulmonary metastases. Nucl Med Biol 2016; 43:773–80.
[17] Vad NM, Kudugunti SK, Graber D, Bailey N, Srivenugopal K, Moridani MY. Efficacy of acetaminophen in skin B16-F0 melanoma tumor-bearing C57BL/6 mice. Int J Oncol 2009;35:193–204.
[18] Vad NM, Yount G, Moore D, Weidanz J, Moridani MY. Biochemical mechanism of acetaminophen (APAP) induced toxicity in melanoma cell lines. J Pharm Sci 2009; 98:1409–25.
[19] Kobayashi M, Hashimoto F, Ohe K, Nadamura T, Nishi K, Shikano N, et al. Transport mechanism of ^{11}C-labeled L- and D-methionine in human-derived tumor cells. Nucl Med Biol 2012;39:1213–8.
[20] Aloj L, Caracó C, Jagoda E, Eckelman WC, Neumann RD. Glut-1 and hexokinase expression: relationship with 2-fluoro-2-deoxy-D-glucose uptake in A431 and T47D cells in culture. Cancer Res 1999;59:4709–14.
[21] Krohn KA, Link JM. Interpreting enzyme and receptor kinetics: keeping it simple, but not too simple. Nucl Med Biol 2003;30:819–26.
[22] Tsao H, Weinstock MA. Visual inspection and the US preventive services task force recommendation on skin cancer screening. JAMA 2016;316:398–400.
[23] Bafounta ML, Beauchet A, Aegerter P, Saiag P. Is dermoscopy (epiluminescence microscopy) useful for the diagnosis of melanoma? Results of a meta-analysis using techniques adapted to the evaluation of diagnostic tests. Arch Dermatol 2001;137:1343–50.
[24] Lassau N, Lamuraglia M, Koscielny S, Spatz A, Roche A, Leclere J, et al. Prognostic value of angiogenesis evaluated with high-frequency and colour Doppler sonography for preoperative assessment of primary cutaneous melanomas: correlation with recurrence after a 5 year follow-up period. Cancer Imaging 2006;6:24–9.
[25] Dancey AL, Mahon BS, Rayatt SS. A review of diagnostic imaging in melanoma. J Plast Reconstr Aesthet Surg 2008;61:1275–83.
[26] Johnson TM, Fader DJ, Chang AE, Yahanda A, Smith 2nd JW, Hamlet KR, et al. Computed tomography in staging of patients with melanoma metastatic to the regional nodes. Ann Surg Oncol 1997;4:396–402.
[27] Jimbow K, Iwashina T, Alena F, Yamada K, Pankovich J, Umemura T. Exploitation of pigment biosynthesis pathway as a selective chemotherapeutic approach for malignant melanoma. J Invest Dermatol 1993;100(Suppl. 2):231S-8S.
[28] Shikano N, Kotani T, Nakajima S, Ogura M, Nakazawa S, Sagara J, et al. Radioiodinated 4-iodo-L-meta-tyrosine, a system L selective artificial amino acid: molecular design and transport characterization in Chinese hamster ovary cells (CHO-K1 cells). Nucl Med Biol 2010;37:903–10.